IEEE Access
Multidisciplinary ⋮ Rapid Review ⋮ Open Access Journal

Received 5 December 2023, accepted 11 January 2024, date of publication 23 January 2024, date of current version 11 March 2024.

Digital Object Identifier 10.1109/ACCESS.2024.3357504

RESEARCH ARTICLE

Optimal Design of Fractional Order Vector Controller Using Hardware-in-Loop (HIL) and Opal RT for Wind Energy System

SHIVAJI GANPAT KARAD[1], RITULA THAKUR[2], MAJED A. ALOTAIBI[3], MOHAMMAD JUNAID KHAN[4], HASMAT MALIK[5,6], (Senior Member, IEEE), FAUSTO PEDRO GARCíA MÁRQUEZ[7], AND MOHAMMAD ASEF HOSSAINI[8]

[1]Instrumentation Engineering Department, Dr. Babasaheb Ambedkar Technological University, Raigad, Lonere 402103, India
[2]Electrical Engineering Department, National Institute of Technical Teachers Training and Research, Chandigarh 160019, India
[3]Department of Electrical Engineering, College of Engineering, King Saud University, Riyadh 11421, Saudi Arabia
[4]Department of Electrical and Electronics Engineering, Mewat Engineering College, Nuh, Mewat 122107, India
[5]Department of Electrical Power Engineering, Faculty of Electrical Engineering, University Teknologi Malaysia (UTM), Johor Bahru 81310, Malaysia
[6]Department of Electrical Engineering, Graphic Era (Deemed to be University), Dehradun 248002, India
[7]Ingenium Research Group, Universidad Castilla-La Mancha, 13071 Ciudad Real, Spain
[8]Department of Physics, Badghis University, Badghis 3351, Afghanistan

Corresponding authors: Majed A. Alotaibi (MajedAlotaibi@ksu.edu.sa), Hasmat Malik (hasmat.malik@gmail.com), and Mohammad Asef Hossaini (asef.hossaini_edu@basu.edu.af)

The authors extend their appreciation to the Researchers Supporting Project at King Saud University, Riyadh, Saudi Arabia, for funding this research work through the project number RSP2023R278. This work was supported in part by the National Institute of Technical Teachers Training and Research (NITTTR) Chandigarh, in part by the All India Council for Technical Education (AICTE) India, and in part by Universiti Teknologi Malaysia (UTM) through the UTM Fundamental Research (UTMFR) Grant under Code Q.J130000.3823.23H05.

ABSTRACT In this paper, a fractional order active (P) and reactive (Q) power controller of doubly fed induction generator (DFIG) is developed and it performance is demonstrated using hardware in loop (HIL) testing with Opal RT OP4510 real-time platform. The DFIG in this paper is modelled using real-time State Space Nodal (SSN) based solver. The Rotor Side Converter (RSC) and doubly fed induction machine are implemented using Opal-RT's ARTEMiS – nodal admittance-based SSN solver which uses smaller time steps than the conventional algorithms to facilitate real-time hardware-in-loop performance analysis of the system. The MATLAB-based FOMCON platform is utilized for designing the proposed fractional order controller. The proposed controller is developed and tested for various dynamic conditions. The performance of conventional proportional integral control and proposed fractional order control using Opal-RT's OP4510 real-time platform is compared. The experimental results demonstrate improved efficiency with the use of proposed fractional order controller.

INDEX TERMS State space nodal (SSN) solver, field oriented control, fractional order controller, optimal control.

I. INTRODUCTION

The cumulative depletion of electrical power and the persistent decay in conventional energy sources resulted into a huge demand and supply gap in electrical power supply. To fulfil this demand and supply gap, alternate Renewable Energy (RE) sources are used to generate electricity. According to a report [1], 3146 GW of worldwide electricity is generated through RE sources in the year 2022. As stated in the Prime Minister's statement at COP26, the ''Ministry of New and Renewable Energy'' is planning to install 500 GW of non-fossil energy capacity by 2030. A 172.72 GW of power from non-petroleum product sources has been introduced in the country as of October 2022. The wind is considered a favourable and prevalent substitute for power generation as it is an extensively distributed and abundantly available

The associate editor coordinating the review of this manuscript and approving it for publication was Ton Duc Do.

resource [2], [3]. According to a report [4], approximately 2/3 of worldwide investment in power plants up-to 2040 will be in renewables and the majority of the share will be in wind energy; as they are the most cost effective source of energy generation. India is 4th in the world for installed capacity of RE sources as well as in wind power generation. As seen in Figure 1, world-wide wind power installation reaches approximately 845 GW in 2022 [5]. India generates approximately 41.2 GW of energy from wind out of 173 GW of total renewables as of October 2022. Figure 2 denotes a graphical representation of wind energy installation in India. A sum of 14.21 GW of sustainable power was added during January to October 2022 when contrasted with limit of 11.9 GW added during the year 2021.

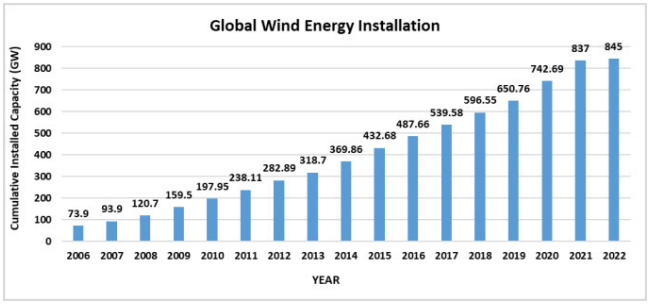

FIGURE 1. Global wind energy installation.

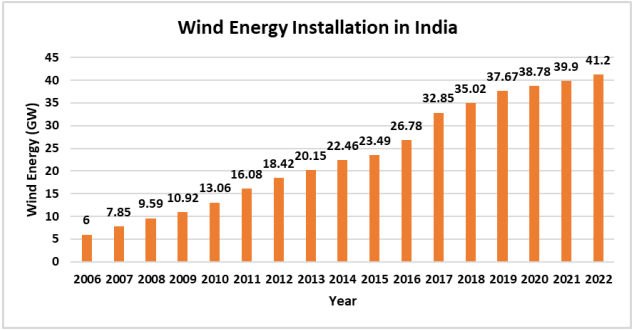

FIGURE 2. Wind energy installation in India.

Taking into consideration the widespread use of small and large sized wind farms having different turbine configurations and advanced trends, it becomes vital to research the issues associated with it such as stability, power quality, reactive power, and reliability. Wind turbines are a clean and sustainable way to generate electricity, but their power output can vary significantly depending on the wind conditions. Effective power control can help to ensure that wind turbines operate efficiently and reliably, even in changing wind conditions. Researcher need to focus on developing new control algorithms that can optimize the power output of wind turbines and ease the grid integration.

Control systems monitor various factors like wind velocity, blade angle, and generator output, and make adjustments to optimize energy production and protect the turbine from damage. Additionally, control systems enable remote monitoring and maintenance, improving the overall performance and lifespan of wind turbines. As wind energy continues to contribute significantly to switch to cleaner and environmentally friendly power generation, effective control strategies are essential to harness its full potential as well as for the growth of the wind energy industry and for achieving a sustainable energy future.

II. RELATED WORK

Wind turbines (WTs) connected to the electric generators are used to generate the electricity from the wind. Owing to the enhanced productivity variable speed WTs are mostly preferred at present for wind power plants. Electric generators are significant part of WTs that is important for energy generation and integration with the grid. Currently, DFIG is extensively preferred for variable wind speed operations in the advanced grid system. DFIGs offer advantages such as minimal expense of converters with four-quadrant and varied speed operational capability when contrasted with fixed speed synchronous generators [6], [7]. The speed of a DFIG Wind Turbine Generator (DFIG-WTG) can be effectively regulated within a range of 67-133% around the synchronous speed by controlling the power flow and direction of the rotor. The management and operation of DFIG systems connected to the grid pose significant challenges due to the complexities involved in regulating the flow of P power and Q power within the grid and DFIG-based wind generation systems (WGS). Some of the state-of-the-art WT concepts and essential power electronic converters and control arrangements are addressed in [8], also author discussed grid necessities and the future technology challenges in WTs.

In the context of DFIG-based WGS, the rotor windings are linked to the grid through a pair of back-to-back Pulse Width Modulation (PWM) converters known as the rotor side converter (GSC) and the grid side converter (GSC). Additionally, the stator windings are directly connected to the grid. A DC link is used in between both of these converters to maintain a constant voltage. When there is a voltage reduction, DC link will take more reactive power from the grid; on the other hand, when there is a voltage increase, it will send reactive power to the grid [9]. The system's effective inertia is impacted by the DFIG's greater penetration, which raises questions about the power system stability [10]. This demands the use of more sophisticated and intelligent control technologies in the WECS control. As found in the literature, the direct torque control (DTC) and vector control (VC) are the two core control methods implemented to accomplish optimal power stabilization of the DFIG [11]. Being a nonlinear control method, DTC adjusts the rotor voltage to an equivalent power by sensing the nonlinear machine parameters such as flux and torque. VC is a linear control strategy which depends upon single input, single output (SISO) type controllers such as PI and PID or a few advance techniques such as sliding mode

control [12]. But the performance of this control mode is subjected to the PI controller tuning, grid voltage conditions and the accuracy in machine parameters [13], [14]. Many other control techniques have been suggested and provided good results for RSC control in the past as observed from the literature review. Yet, there are many challenges involved such as nonlinear effects, unmodelled dynamics, parameter variations and unknown disturbances [15], [16].

Direct VC with fuzzy sliding mode control with space vector modulation inverter [17] has been applied to control reactive and stator active power and shows improved performance. Direct stator VC using field oriented control (FOC) technique with PI-hysteresis controller strategy is used for control of standalone WECS in [18] shown effectiveness against parameter variations. The second order SMC strategy proposed in [19] for the control of DC link voltage based on vector control gives enhanced response against uncertainties, parametric variations and unidentified disturbances in the system. The coordinated control approach [20], [21] used to improve transient stability can also enhance the control economy when engaged for power control in synchronous generator and DFIG. Linear quadratic regulator (LQR) based optimal preview controller (OPC) proposed in [22] for stator PQ control of a DFIG based WT system. The control technique has undergone testing for both sub-synchronous and super-synchronous operation using stator voltage-oriented control (SVOC). The paper [23] discusses different control strategies that are employed to enhance the efficiency and reliability of wind energy systems based on DFIGs.

Though various modern infrastructure and control methods have been developed and used in the current wind farms, yet there are few technical challenges that must be addressed such as grid integration, power quality, stability, LVRT Control, frequency control and management, etc. Due to the increased penetration of wind power into the grid voltage and frequency instability issues are the most important challenges required to be addressed. The Iceland operation is also one of the important challenge from dc link voltage control point of view.

A sort of computer simulation known as real-time simulation in which the simulation model runs at the speed of real world processes that it is simulating. It calculates and updates the simulation results in a time frame that closely resembles or equals the rate at which events occur in the physical system being simulated. Recently, Real Time Digital Simulation (RTS) is becoming an efficient tool for electrical power systems simulation in the research and development as well as control of the electrical power system. Real-time simulation often requires specialized simulation engines and hardware, including high-performance computing clusters or GPUs, to achieve the necessary computational speed and accuracy. With the development of high-speed platforms and improved computational capability, these technologies make power electronic converter research possible. Also, they are useful for rapid control prototyping, testing and investigation of fault and protection [24]. As the RTS system uses dedicated high speed processors and hardware it is possible to simulate the system as a real time system as it operates physically. The RTS runs at a fixed time-step interims (Ts), in which, the system reads the inputs and performs essential calculations so that to generate all the outputs. But in some cases there may be chances of overrun due to the constraint of fixed time step Ts, when the time required to perform the calculation is more than the Ts and real time simulation may miss the synchronization. The HIL based real time simulation has been used effectively in various power system application such as DFIG control [25], grid integration [26], multilevel converter control [27], Fault analysis in IEEE-9 bus system [28], analysis of IEEE-5 bus system [29], and stator fault improvement in PMSM [30].

The motivation of this research paper that demonstrates the applicability of novel fractional order PI controller to control the nonlinear wind power system with DFIG is to mitigate the challenges associated with the traditional controller and implement it using real time simulation environment. Fractional calculus is becoming one of the more effective and comprehensive solution for controlling the nonlinear integer order as well as fractional order systems.

In most of the present control schemes, parameter uncertainty, nonlinear nature of wind turbine and power quality still remains the main challenges. So there is need to design non-linear controller for controlling wind energy conversion system. Most of the control schemes use conventional PI regulator in current control or voltage control loop that is not effective to handle the nonlinearity and parametric uncertainties. The fractional order controllers have been applied in non-linear control system applications for MPPT as well as power control loops in DFIG based WT.

The design of an optimal fractional order controller for RSC control of DFIG based wind turbine system and implementation of proposed control scheme using Opal-RT's OP-4510 real time digital simulator for enhanced control performance with increased output power efficiency is the major contribution of this paper. This paper aims to investigate and evaluate the effectiveness of vector control strategy used to control rotor side converter control implemented using Opal-RT's CPU based toolbox ARTEMiS with lower time step in association with MATLAB/Simulink Simscape Electrical library. A summary of related work is represented in Table 2.

Remaining of the paper is organized as: section III describes the operation of DFIG based WT system, section IV describes the implementation of proposed control strategy using real time platform and ARTEMiS-SSN solver with experimental setup, simulations results and analysis. The conclusion and the future work scope are provided in section V.

III. OPERATION OF DFIG ASSISTED WIND TURBINE

Schematic configuration of DFIG–WECS represented by Figure 3 mainly comprises of a WT, DFIG, power electronics circuits and associated control devices with supportive mechanical systems though not shown in detail in the diagram. The DFIG-WECS configuration employs wound rotor

induction generator, where stator is connected to the power grid, whereas the rotor is joined to the grid through RSC and a GSC using slip rings. Due to this setup, DFIG is able to receive and send power from the grid [29]. The stator windings pump the power into the grid. This power flow in the DFIG depends on the operating mode of DFIG as motor mode or generator mode.

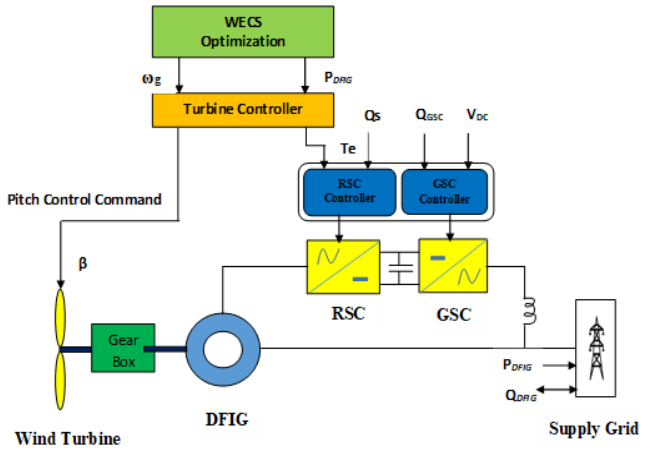

FIGURE 3. DFIG based WECS.

Mathematical models are essential in the initial design phase of wind turbines. the DFIG-WTs play a significant role in modern power systems, and their dynamic behavior has a direct impact on system stability. Mathematical models allow for the study of the DFIG-WT's response to disturbances, helping to assess and improve the stability of the grid. Also, DFIG-WTs can actively control voltage and frequency. Mathematical models are used to design and test these control schemes, ensuring that DFIG-WTs provide stable and reliable grid support. Through the subsequent subsection mathematical model for WT and DFIG with stationary reference frame are described in detail.

A. DYNAMIC DQ MODELLING OF DFIG

Vector control can help to improve the efficiency of DFIG-based WTs by minimizing the torque ripples. Vector control can be applied to optimize the output power of a WT by controlling the rotor speed and torque. This can help to maximize the amount of energy that can be extracted from the wind. For correct perception and creating vector control strategies in a wind turbine system, it is crucial to be knowledgeable about the DFIG's dynamic model. Vector control can be used to synchronize a WT to the grid. This is necessary for the turbine to be able to safely export its power to the grid. A model of an electrical machine must take into account all dynamic effects that could result from both steady-state and transient operations. For constructing the decoupled active and reactive power regulator system, the dynamic model of the DFIG is also necessary. Figure 4 below shows the DFIG's electrical analogue circuit in synchronous reference frame.

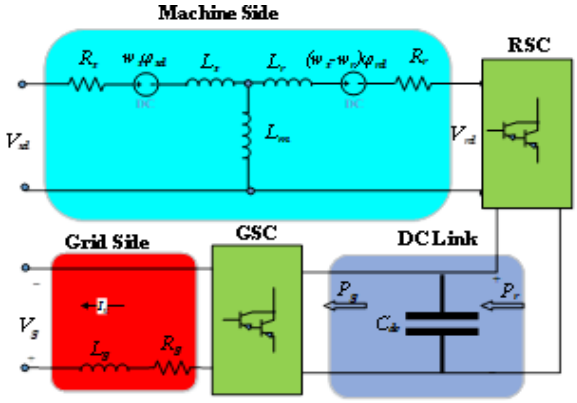

FIGURE 4. DFIG electrical equivalent circuit.

The most common mathematical model used to represent the machine's dynamic behaviour is one with a dq synchronous rotating reference frame. The rotor and stator voltage equations are expressed as [31]:

$$\left.\begin{aligned}\varphi_{sd} &= \varphi_s \\ \varphi_{sq} &= 0\end{aligned}\right\} \tag{1}$$

Hence, the torque equation becomes,

$$T_e = P\varphi_{sd} i_{xq} \tag{2}$$

The equations for the currents, fluxes, and voltages are stated as follows if the stator flux orientation hypothesis is true and the stator phase resistance is ignored.

$$\left.\begin{aligned}V_{sd} \approx p\varphi_{sd} &= p\varphi_s = 0 \\ V_{sq} \approx \omega_s \varphi_{sd} &= V_s\end{aligned}\right\} \tag{3}$$

$$\left.\begin{aligned}\varphi_s \quad & L_s i_{rd} + L_m i_{rd} \\ 0 &= L_s i_{rq} + L_s i_{r\rho}\end{aligned}\right\} \tag{4}$$

Using equation (3) and (4), we can have relationship between stator current and rotor current as:

$$\begin{aligned} i_{sd} &= \frac{\varphi_s}{L_s} - \frac{L_m}{L_s} i_{rd} \\ i_{sq} &= -\frac{L_m}{L_s} i_{rq} \end{aligned} \tag{5}$$

Similarly, active and reactive power along with the electromagnetic torque is expressed in dq reference frame as:

$$\left.\begin{aligned}P_s &= V_s i_{sq} \\ Q_s &= V_s i_{sd}\end{aligned}\right\} \tag{6}$$

$$T_e = p\varphi_s \frac{L_m}{L_s} i_{rq} \tag{7}$$

Now by substituting the currents using equation (5) in equation (6), we have

$$\begin{aligned} P_s &= -V_s \frac{L_m}{L_s} i_{sq} \\ Q_s &= \frac{V_s \varphi_s}{L_s} - \frac{V_s L_m}{L_s} i_{rd} \end{aligned} \tag{8}$$

The rotor side dq components i_{dr} and i_{dq} can also be obtained by considering the stator reference frame and

expressed as in the following set of equations. We can get the stator voltage orientation relative to the reference frame along the q-axis without taking into account the stator resistance [32], [33].

$$V_{rd} = \left(R_r + \sigma L_r \frac{d}{dt}\right) I_{dr} - (w_s - w_r)\,\sigma L_r I_{rq} + \frac{L_m}{L_s}(V_{sd}) \tag{9}$$

$$V_{rq} = (w_s - w_r)\,\sigma L_r I_{rd} + \left(R_r + \sigma L_r \frac{d}{dt}\right) I_{rq} - + \frac{L_m}{L_s}(V_{sq} - w_r \varphi_{sd}) \tag{10}$$

where $\sigma = 1 - \frac{L_m^2}{L_s L_r}$

By expressing the above in matrix from,

$$\begin{bmatrix} V_{rd} \\ V_{rq} \end{bmatrix} = \begin{bmatrix} R_r + \sigma L_r \frac{d}{dt} & -(w_s - w_r)\sigma L_r \\ (w_s - w_r)\sigma L_r & R_r + \sigma L_r \frac{d}{dt} \end{bmatrix} \begin{bmatrix} V_{rd} \\ V_{rq} \end{bmatrix} + \frac{L_m}{L_s} \begin{bmatrix} V_{sd} \\ V_{qs} - w_r \varphi_{sd} \end{bmatrix} \tag{11}$$

In a similar vein, the (d-q) components of rotor currents are utilized to calculate the total real and reactive power of the rotor as:

$$\begin{bmatrix} P_t \\ Q_t \end{bmatrix} = \begin{bmatrix} 0 & \frac{3}{2}(s-1)\frac{L_m}{L_s} V_s \\ \frac{3}{2}(s-1)\frac{L_m}{L_s} V_s & 0 \end{bmatrix} \begin{bmatrix} I_{rd} \\ I_{rq} \end{bmatrix} + \begin{bmatrix} 0 \\ \frac{3}{2}\frac{V_s \varphi_s}{L_s} \end{bmatrix} \tag{12}$$

As seen from (12), monitoring the rotor current, the overall PQ power can be managed as [32]:

$$\begin{bmatrix} I_{rd}^* \\ I_{rq}^* \end{bmatrix} = \begin{bmatrix} 0 & \frac{3}{2}(s-1)\frac{L_m}{L_s} V_s \\ \frac{3}{2}(s-1)\frac{L_m}{L_s} V_s & 0 \end{bmatrix}^{-1} \times \left\{ \begin{bmatrix} P_{rd}^* \\ P_{rq}^* \end{bmatrix} - \begin{bmatrix} 0 \\ \frac{3}{2}\frac{V_s \varphi_s}{L_s} \end{bmatrix} \right\} \tag{13}$$

where $*$ denotes the reference of values.

The torque equation (7) can also be used to calculate the rotor mechanical power output.

$$\mathrm{P_{mec}} = \mathrm{T_{em}}\omega_\mathrm{r} = -\frac{3}{2}\mathrm{p}\frac{\mathrm{L_m}}{\mathrm{L}_s}\varphi_s \mathrm{i_{rq}}\omega_\mathrm{r} \tag{14}$$

Considering the total mechanical power output and the total electrical power, the efficiency of the DFIG can also be calculated as [33]:

$$\text{Efficiency}\,(\eta) = \frac{\mathrm{P_{mec}}}{\mathrm{P_s} + \mathrm{P_r}} X 100\% \tag{15}$$

B. RSC CONTROL

The sophisticated and crucial RSC control is a feature of variable-speed WTs and other applications. To increase the effectiveness, dependability, and grid integration capabilities of RSC systems, cutting-edge control algorithms and technologies are constantly being developed. Optimisation and control of the WECS is one of the difficult tasks that is directly related to the output and stability of the system. RSC controls the decoupling of active and reactive power, while GSC controls the DC link voltage in accordance with the amount and flow of power. The RSC need to be capable to deliver at least 30% of the stator voltage in order to deliver at least 30% of the generator ratings because the slip of the DFIG is often limited between −0.3 and 0.3 [34]. This paper aims to study the performance of VC based RSC control strategy using eHS based power hardware converters using real time simulation structure. The most popular approach to constructing RSC controls utilizing a field-oriented vector control scheme was covered in this section. The [35] contains the RSC's vector control strategy for a stator flux-oriented reference frame. To autonomously regulate the PQ power of the rotor with stator voltage or flux orientation approach based standard PI control is typically used. The block schematic of RSC control is illustrated in Figure 5.

The current and voltage loops can be controlled using a variety of control techniques, as identified and researched in the literature. Owing to its simple structure and ease of adjustment, the traditional PI regulator is the most popular. The dq reference frame model's above-described relationship between rotor voltages and currents is used to develop the PI regulator. In DFIG, the PQ power is managed by monitoring the rotor currents, as shown in figure 5 and described in (16). The PI control can be determined from the rotor current dynamics (16) as defined in [36]:

$$\left.\begin{aligned} V_{rd}^* &= K_{p1} e_d + K_{i1} \textstyle\int e_d d\tau - (\sigma L_r s \omega_s I_{rq} + \frac{R_s L_m}{\omega_s L_s} V_s) \\ V_{rq}^* &= K_{p2} e_q + K_{i2} \textstyle\int e_q d\tau - (\sigma L_r \omega_s I_{rd} + \frac{s L_m}{L_s} V_s) \end{aligned}\right\} \tag{16}$$

where, $e_d = (I_{rd}^* - I_{rd})$ and $e_q = (I_{rq}^* - I_{rq})$,

K_{p2} and K_{i2} – gains of interior current loop,

K_{p1} *and* K_{i1} – gains for exterior current loop.

These parameters are set in the control system to achieve quick reaction. For FOPI controller order of integration also need to be set for achieving the more effective response.

C. DESIGN OF FRACTIONAL ORDER CONTROLLER

Control systems play a fundamental role in regulating the behavior of various processes and ensuring they perform optimally. Traditionally, control theory has predominantly relied on integer-order differential equations to model and design controllers for these systems. In recent years, there has been a notable movement in the field of control engineering, marked by the emergence of Fractional Order Control (FOC). The FOC is an innovative methodology that expands the scope of control theory beyond traditional integer-order calculus. It achieves this by integrating fractional-order calculus principles into the design and analysis of control systems.

The FOC, alternatively referred to as calculus of fractional derivatives and integrals, extends the conventional integer-order calculus by accommodating non-integer (fractional) orders of differentiation and integration.

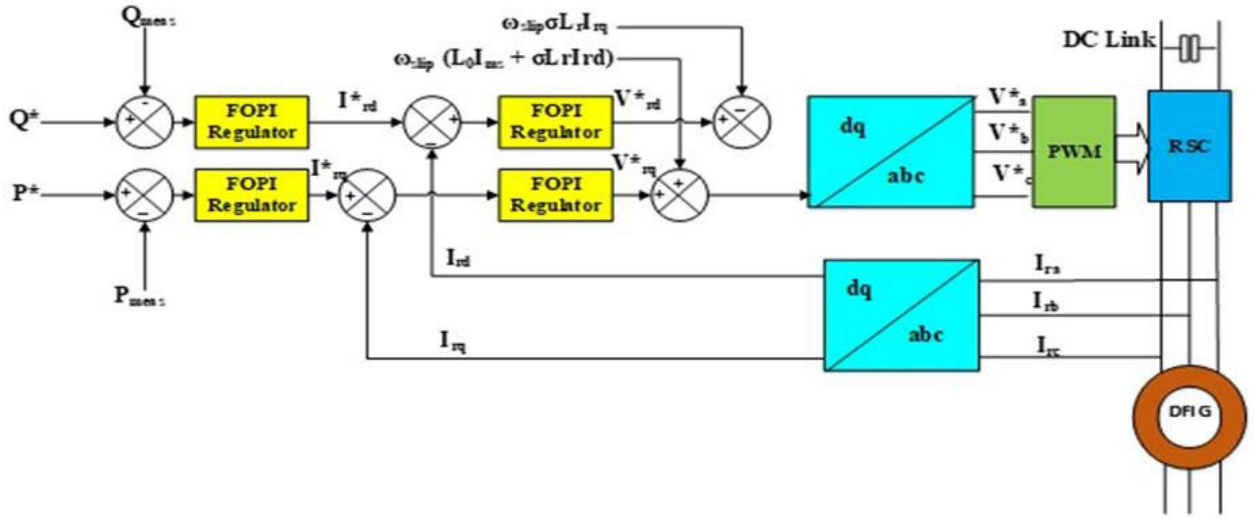

FIGURE 5. RSC vector control structure.

The incorporation of fractional calculus principles in the fractional order PID (FOPID) control methodology allows it to offer equivalent functionality to that of a conventional PID controller. Fractional calculus is a mathematical framework that introduces the concept of non-integer integration and differentiation operators denoted as ${}_aD_t^{\alpha}$, where a and t represent the bounds of integration or differentiation, and $\alpha \varepsilon R$ belongs to the set of real numbers. The mathematical expression and various definitions of this operator are discussed in [37]. The continuous differ-integral operator expresses the extrapolation of differentiation and integration to any order as [38]:

$$ {}_aD_t^{\alpha} = \begin{cases} \dfrac{d^{\alpha}}{dt^{\alpha}} R(\alpha) > 0 \\ 1R(\alpha) = 0 \\ \displaystyle\int_a^t (d\tau)^{\alpha} R(\alpha) < 0 \end{cases} \tag{17} $$

In this expression "a" stands for the integration's lower bound, "α" for the order of fractional differentiation or integration, and "$+\alpha$" and "$-\alpha$" symbolizes integration and differentiation respectively. There are two definitions of fractional order diffe-integral that are often used in the literature: Grunwald-Letnikov (GL) and Riemann-Liouville (RL).

The GL definition is given as [38]:

$$ {}_aD_t^{\alpha} f(t) = \lim_{h \to 0} h^{-\alpha} \sum_{j=0}^{\frac{t-a}{h}} (-1)^j \binom{\alpha}{j} f(t - jh) \tag{18} $$

where h is the time step.

The following is the RL definition:

$$ (t) = \frac{1}{\Gamma(n - \alpha)} \left(\frac{d^n}{dt^n}\right) \int_a^t \frac{f(\tau)}{(t - \tau)^{\alpha - n + 1}} d\tau \tag{19} $$

In reference [39], a FOPID controller has been introduced, which incorporates five tuning parameters: proportional gain, integral gain, derivative gain, order of integration, and order of differentiation. The efficacy of this newly developed controller surpasses that of the integer PID controller for both integer order systems and fractional order systems [40]. A continuous domain FOPID is expresses as:

$$ C(s) = K_P + \frac{K_I}{s^{\lambda}} + K_D s^{\mu} \tag{20} $$

where, C(s) is the transfer function controller with K_P, K_I, and K_D be the gains, λ is integration order and μ as the order of differentiator.

Various approaches are taken into consideration when designing a FOC. The paper [41] presents a discussion on the design, tuning, and optimization of fractional order control using the FOMCON toolkit. The study employed the approach of retuning the current PI or PID controller [42] to create the FOPI controller for the vector control of DFIG machine. Beauty of this technique is that, it allows fractional order dynamics to be integrated into an integer order PID without changing the loop. It basically adds another loop with retuning FOPID into the existing system. Following proposition is applied to form the correlation between the controller parameters [43].

The time domain and frequency domain are the two approaches for designing the fractional order controller. Optimal fractional order controller is designed for achieving better stability, minimizing the response time of the system and disturbance rejection. Optimal design also helpful in reducing the errors with enhanced system response.

Proposition 1: Consider the conventional PID controller expressed by [43]:

$$ C_{PID}(s) = K_P + K_I s^{-1} + K_D s \tag{21} $$

$$C_{PID}(s) = K_P + K_I s^{-1} + K_D s \tag{22}$$

Let $C_R(s)$ be a controller of the form

$$C_R(s) = \frac{K_2 s^{\beta} + K_1 s^{\alpha} - K_D s^2 + (K_0 - K_P)s - K_I}{K_D s^2 + K_P s + K_I} \tag{23}$$

where $-1 < \alpha < 1$ and $1 < \beta < 2$. The resulting FOPID, $PI^{\lambda}D^{\mu}$ have the coefficients as

$$K_P^* = K_0,\ K_I^* = K_1,\ \text{and}\ K_D^* = K_2$$

and the orders will be

$$\lambda = 1 - \alpha, \quad \mu = \beta - 1$$

So the overall feedback becomes of the form

$$C(s) = (C_R(s) + 1).C_{PID}(s) \tag{24}$$

The parameters of the retuning controller can be estimated from those of FOPID controller [44]. Therefore, with this proposed returning method the original closed-loop system functions as earlier, but with enhanced performance due to the introduced reference signal dynamics in it. Design and implementation of the proposed controller is foremost important task in applying it in various applications. Rewriting equation (24) we have

$$C_R(s) = \left(\frac{K_2}{D(s)}\left[s^{\beta}\right]\right) + \left(\frac{K_1}{D(s)}\left[s^{\alpha}\right]\right) - \left(\frac{K_D s^2 - (K_0 - K_P)s + K_I}{D(s)}\right) \tag{25}$$

where $D(s) = K_D s^2 + K_P s + K_I$ and [.] is Oustaloup approximations. Equation (25) is used to implement the controller as given in [43].

Proposed fractional order controller when used for the DFIG based WT system under study provide better and more accurate results due the representation of system in non-integer order dynamics. Also, it is more flexible in tuning the controller parameters than the conventional integer order controller that proves to be beneficial in improving the transient response of the system. It is demonstrated that a promising control technique for the reliable and effective regulation of dynamics systems with model uncertainties is the fractional order control approach.

D. MODEL OF DFIG USING SSN SOLVER

The majority of the solvers used for RTS are imitation-based and based either on full state-space systems, as in SimPower Systems (SPS) and the eMEGAsim real-time simulator from Opal-RT or the nodal admittance approach with trapezoidal discretization, as in Hypersim or RTDS real-time simulators. The SSN solver uses arbitrary sized clusters of electrical components defined by state-space equations and is based on the Electromagnetic Transients Programme (EMTP) nodal admittance approach [45]. For a generalised branch or SSN group made out of electrical components coupled to an unknown voltage/current terminal, the state space equations can be written as [45]:

$$\left.\begin{aligned} x' &= A_k x + B_k u \\ y &= C_k x + D_k u \end{aligned}\right\} \tag{26}$$

where, x denotes the system's states, u denotes inputs, y denotes output and Ak, Bk, Ck, Dk denote state space matrices corresponding to the k-th permutation. After discretizing these equations becomes (27), as shown at the bottom of the next page, where, A_d, B_{d1}, B_{d2}, C and D are the discrete state matrices,

$u_{(in)}$ and $u_{(uk)}$ are internal and unknown source of state space model

$y_{(in)}$ is internal output of model

$y_{(uk)}$ is the nodal output of state space model

Further mathematical processing with different discretization rules such as trapezoidal or Backward-Euler these sets of equations are transformed to Nortan type discrete companion model (DCM) or Thevenin type DCM. The SSN model for an induction machine (IM) is derived using fixed d-q (Park) transformation. Using the Park transformation with the assumption $\theta = 0$ for stator quantities and $\theta = -\theta_{\text{rotor}}$ for rotor quantities, voltage and current for induction machine leads to [45]:

$$\begin{aligned} V_{dqs} &= T.V_{abcs} & I_{abcs} &= T^t.I_{dqs} \\ V'_{dqr} &= {}^{ns}\!/_{nr}\, T.V_{abcr} & I'_{abcr} &= {}^{ns}\!/_{nr}\, T^t.I_{dqr} \end{aligned} \tag{28}$$

where, ${}^{ns}\!/_{nr}$ is the stator to rotor turns ratio, suffix s and r stands for stator and rotor respectively. T is the park transformation given as:

$$T = S\sqrt{\frac{2}{3}}\begin{bmatrix} 1 & -1/2 & -1/2 \\ 0 & \sqrt{3}/2 & -\sqrt{3}/2 \end{bmatrix} \tag{29a}$$

where

$$S = \begin{bmatrix} \cos(\theta) & \sin(\theta) \\ -\sin(\theta) & \cos(\theta) \end{bmatrix} \tag{29b}$$

The machine equations can be written as:

$$\hat{\varphi} = \left(-RL^{-1} + \Omega\right)\varphi + V_{dq} \tag{30}$$

$$\hat{\varphi} = \left(-RL^{-1} + \Omega\right)\varphi + V_{dq} \tag{31}$$

with

$$V_{dq} = \begin{bmatrix} V_{sd} & V_{sq} & V'_{rd} & V'_{rq} \end{bmatrix}^t,$$
$$\varphi = \begin{bmatrix} \varphi_{sd} & \varphi_{sq} & \varphi'_{rd} & \varphi'_{rq} \end{bmatrix}^t$$
$$R = \text{diag}(R_s, L_s, R'_r, L'_r),$$
$$\Omega = \begin{bmatrix} 0 & 0 & 0 & 0 \\ 0 & 0 & 0 & 0 \\ 0 & 0 & 0 & -\omega_e \\ 0 & 0 & \omega_e & 0 \end{bmatrix}$$

where

ω_e, the rotor electrical frequency is given by $\omega_e = \text{pp}.\ \omega_m$,

ω_{m-} rotor speed in rad/s

pp - number of pole pairs and,

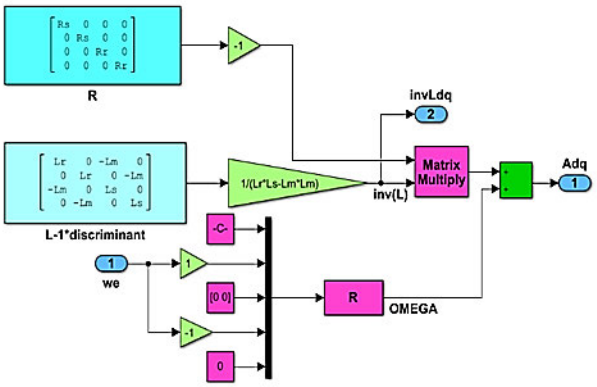

FIGURE 6. Matrices subsystem in simulink.

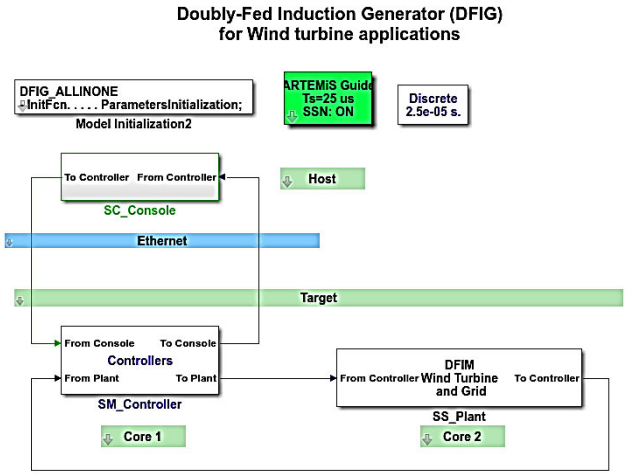

FIGURE 7. Simulink top level schematic for real time simulation.

R_s, L_s, - stator resistance and inductance
R'_r, L'_r – rotor resistance and inductance
Similarly,

$$L^{-1} = \frac{1}{L'_r L_s - L_m^2} \begin{bmatrix} L'_r & 0 & -L_m & 0 \\ 0 & L'_r & 0 & -L_m \\ -L_m & 0 & L_s & -\omega_e \\ 0 & -L_m & 0 & L_s \end{bmatrix} \tag{32}$$

The phase-domain equations of the IM are used to derive the SSN - DCM equations, which provide a time-variant model for the IM. Figure 6 displays the Simulink matrices subsystem. In the ARTEMiS SSN solver is generally implemented using Simulink 'Sfunction Builder' blocks. It is also possible to implement it directly into a 'C' code S-function. The key challenge is to synchronize the many algorithmic steps of SSN within Simulink's simulation because each block's outputs must be updated first, then its internal states.

IV. IMPLEMENTATION OF DFIG-WT SYSTEM IN REAL TIME

Figure 7 shows the top level schematic of complete Simulink model developed in MATLAB grouped into three important subsystems namely Master subsystem (SM_Controller), Slave subsystem (SS_Plant) and Console subsystem (SC_Console). The SM_Controller subsystem consists of the various controllers required for the control of RSC, GSC, DC link, Speed etc.

The SS_Plant is the SSN based model of DFIG named as a plant whereas the SC_Console includes all the scopes and setting which can be viewed through console panel. The SM_Controller and SS_Plant after building the real time model using RT-LAB are loaded to the OP4510 CPU core so that they can run in real time mode while the SC_Console subsystem runs on the host PC so that the setting can be changed while simulation is running and also performance of the system through scope.

A. RT-LAB™ SIMULATION WORKBENCH

In this study, Simulink models are integrated with MATLAB/Simulink®so that they can interact with the real environment in real-time. This is made possible through the use of RT-LAB 2020.4.1. This multi-domain platform integrates with many other programming environments and offers adaptable and scalable solutions for applications in electrical systems, aerospace, electrical vehicles, etc. Through its console panel, it also manages code creation and an interactive interface and offers online parameter change similar to a physical real-time system. Some of the software libraries offered to build the model in conjunction with Simulink model to execute it in real-time environment are RT Lab IO, RTE, ARTEMiS, eMEGASIM, and eFPGASIM.

In this study, the performance of the DFIG control is evaluated in real time using ARTEMiS, a CPU-based Electrical Toolbox designed to interface with Simscape ElectricalTM. For the consistent, accurate, and fixed time step computations required for real-time simulations, it provides enhanced solvers and algorithms. Additionally, ARTEMiS maintains the model's validity thanks to an effective decoupling technique without the need of any artificial delays. For real-time simulation, ARTEMiS provides specialized models

$$\left.\begin{aligned} x_{n+1} &= A_d x_n + B_{d1} u_n + \begin{bmatrix} B_{d2(in)} & B_{d2(uk)} \end{bmatrix} \begin{bmatrix} u_{n+1(in)} \\ u_{n+1(uk)} \end{bmatrix} \\ \begin{bmatrix} y_{n+1(in)} \\ y_{n+1(no)} \end{bmatrix} &= \begin{bmatrix} C_{(in)} \\ C_{(uk)} \end{bmatrix} x_{n+1} + \begin{bmatrix} D_{(in,in)} & D_{(in,uk)} \\ D_{(uk,in)} & D_{(uk,uk)} \end{bmatrix} \begin{bmatrix} u_{n+1(in)} \\ u_{n+1(uk)} \end{bmatrix} \end{aligned}\right\} \tag{27}$$

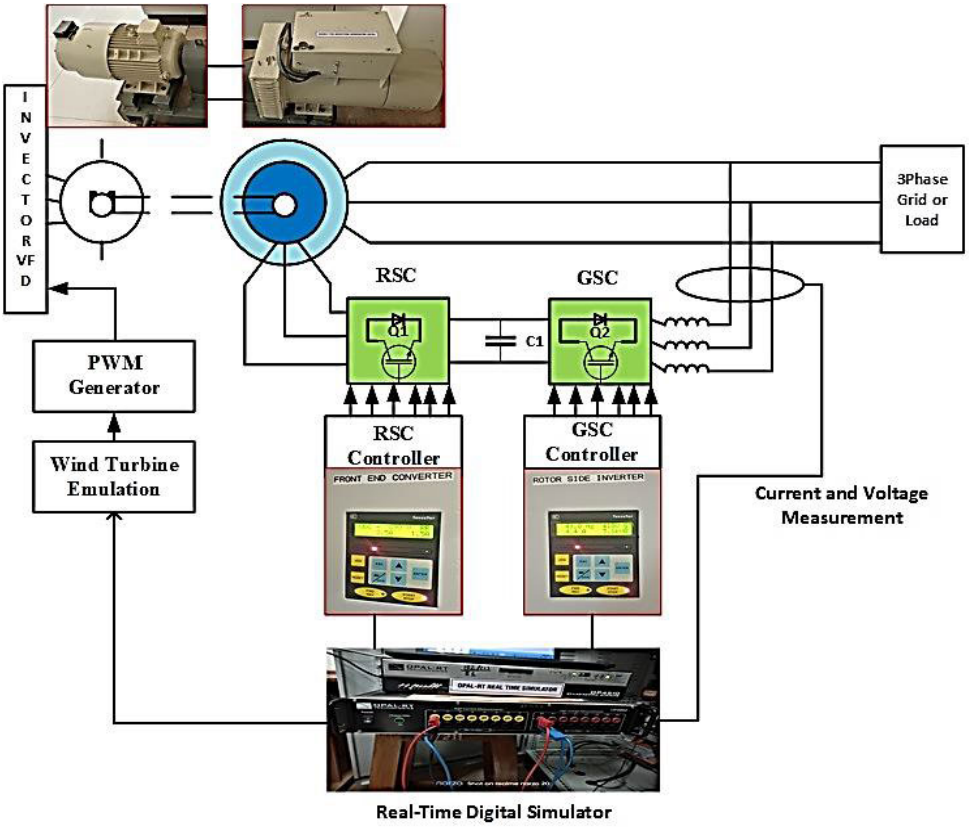

FIGURE 8. DFIG experimental setup.

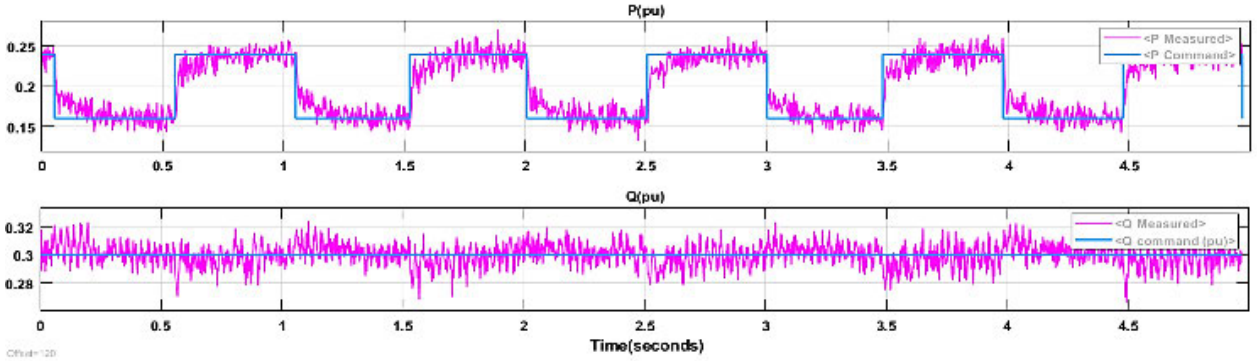

FIGURE 9. PQ response with PI controller.

like ARTEMiS Distributed Parameter Line and ARTEMiS Stublines that conduct distributed power system simulation using RT-LAB.

B. SIMULATION RESULTS WITH HIL

The experimental simulation is performed to demonstrate and study the effective applicability of proposed controller by using OPAL-RT real time digital simulation and laboratory experimental setup of DFIG machine. It has been seen that the HIL simulation is very much closer to the actual working conditions. The HIL simulation is an effective way of analyzing the performance of controller by simulating the controller in rapid control prototyping configuration with the help of real time simulators. The experimental setup using OP4510, OP8662 and a DFIG based wind emulator is shown in Figure 8.

The simulation results for conventional PI controller based rotor side converter control scheme has been shown in Figure 9 to Figure 11 and same with the proposed FOPI has been shown in the Figure 12 to Figure 15.

In this experimental setting, the reactive power is managed by maintaining a constant value of the d-axis rotor

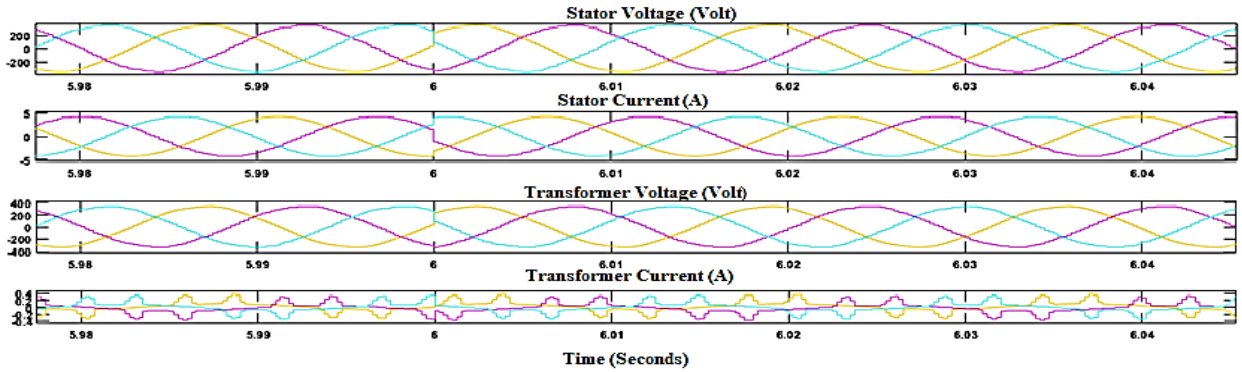

FIGURE 10. Zoomed response of stator voltage and current with PI controller.

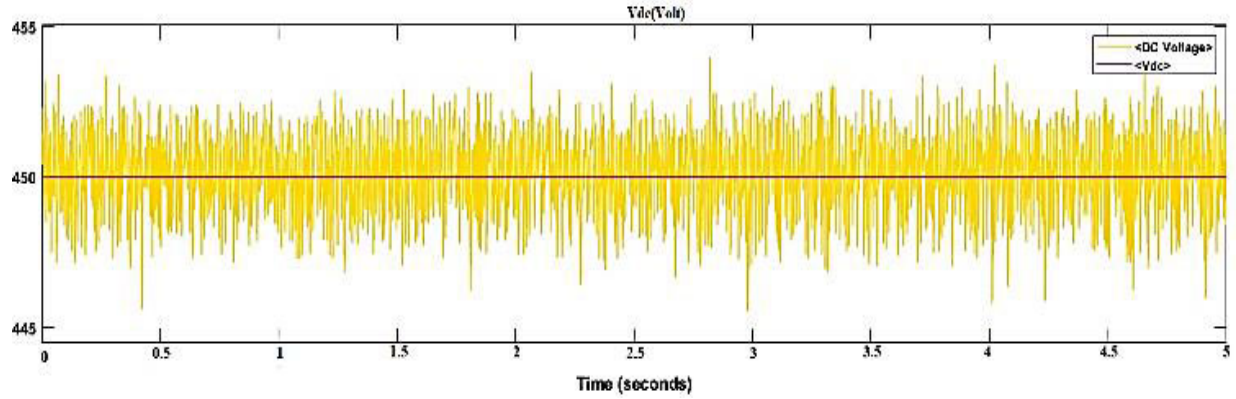

FIGURE 11. DC link voltage with PI controller.

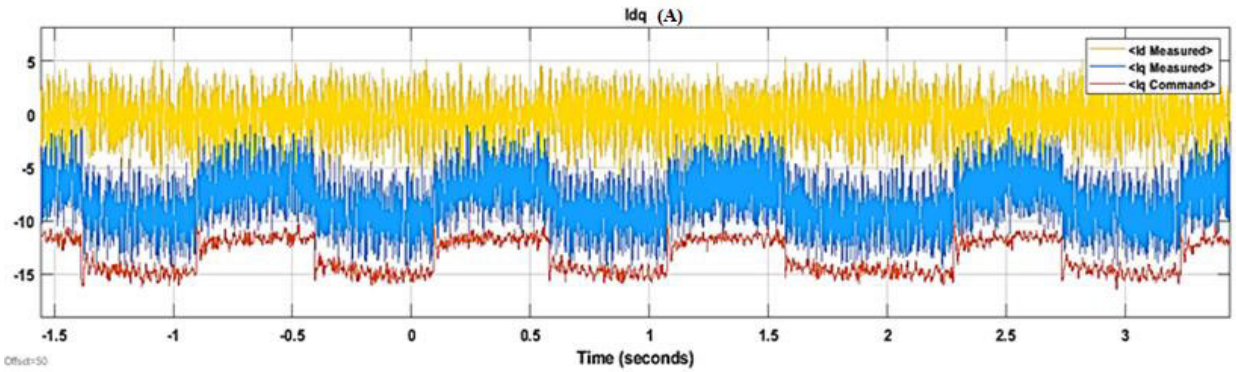

FIGURE 12. Rotor dq-current response with FOPI.

current while the active electrical power is regulated by modulating the q-axis rotor current. Figure 9 as well as Figure 13 demonstrates that, the rotor currents I_{rd} and I_{rq} are tuned to control overall response of active and reactive power. The reactive power that will either be transmitted to the grid or consumed by the grid is clearly controlled by the rotor d-current. The generated active power that DFIG transmits to the grid is managed by the rotor q-current. The tracking performance is also well-established, as can be seen.

The response of DC link voltage is illustrated in Figure 11 and Figure 14 with conventional controller and proposed fractional order controller respectively. The response with real time simulation has been observed more discrete due to use of real time solver with fixed time step. The stator voltage and current responses are also presented in Figure 10 and

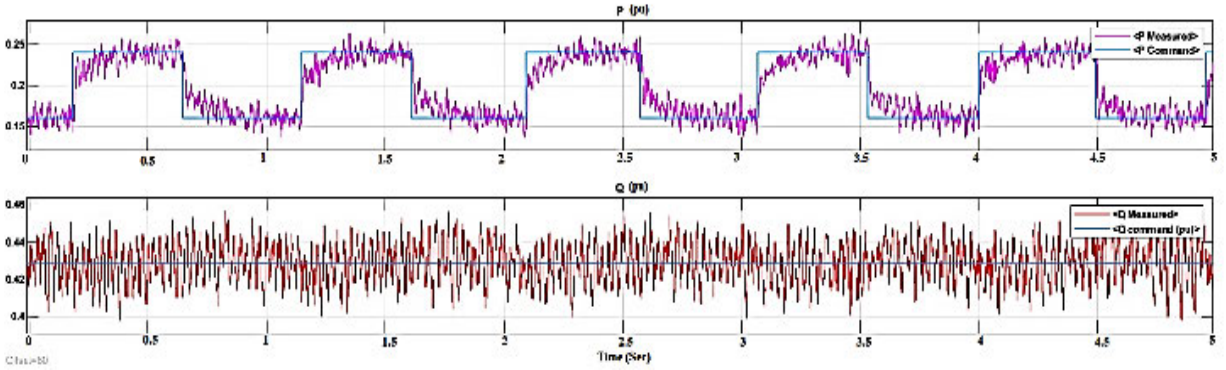

FIGURE 13. PQ tracking response with FOPI controller.

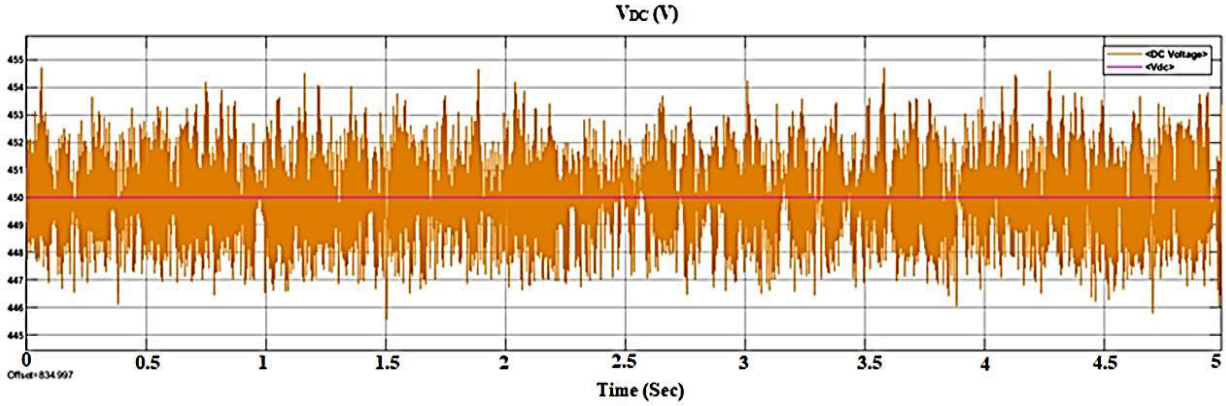

FIGURE 14. V_{DC} with FOPI controller.

Figure 15 with PI and FOPI controllers and that matches with the simulation results obtained with the offline simulation.

C. EXPERIMENTAL VALIDATION AND RESULTS

The suggested control approach is validated on a laboratory-based experimental test bench with a DFIG coupled with an induction motor as a wind speed emulator and a real-time simulator in order to compare its performance to that of a conventional controller and confirm its design. OPAL-RT's OP4510 real time simulator has been used to integrate the controller with experimental hardware and the MATLAB/SIMULINK and RT-LAB real time simulation environments. In order to control the active and reactive power of a 6 KVA DFIG-based wind turbine system with parameters as mentioned in Table 2 in Appendix A. The DFIG and induction motor drive specifications are specified in Table 3 in Appendix B and Table 4 in Appendix C respectively.

The experimentation is carried out to measure the PQ power with the conventional controller by measuring actual output voltage and current signals and calculating the power. The measured power is compared with the ideal power of the DFIG for both the controller schemes. The experimentation is performed by keeping reactive power zero and controlling the active power only. The experimental results obtained on the 6KVA laboratory based DFIG testbed with PI and proposed FOPI controller are plotted in Figure 16 and 17. It is evident from the plots that the due the added advantages of proposed fractional order PI controller such as better robustness and speed tracking response it shows improved performance than that of the conventional PI controller.

TABLE 1. Comparison of total output power and efficiency with PI and FOPI Controller.

Wind Speed (m/s)	Mechanical Power (KW)	Total Power with PI (W)	Efficiency (%)	Total Power with FOPI (W)	Efficiency (%)
3	3.1	2.3	**71.3**	2.5	**80.6**
4	3.4	2.5	**73.5**	2.8	**82.4**
5	4.9	3.0	**76.9**	3.24	**83.1**
6	4.33	3.6	**83.1**	3.9	**90**
7	4.41	3.7	**83.9**	4.0	**90**
8	4.73	3.9	**80.7**	4.2	**88.8**
9	5.0	4.0	**80**	4.3	**86**
10	5.0	4.1	**82**	4.4	**88.6**
11	5.66	4.5	**79.5**	4.5	**90.1**
12	6.66	5.5	**82.5**	6.2	**93.1**

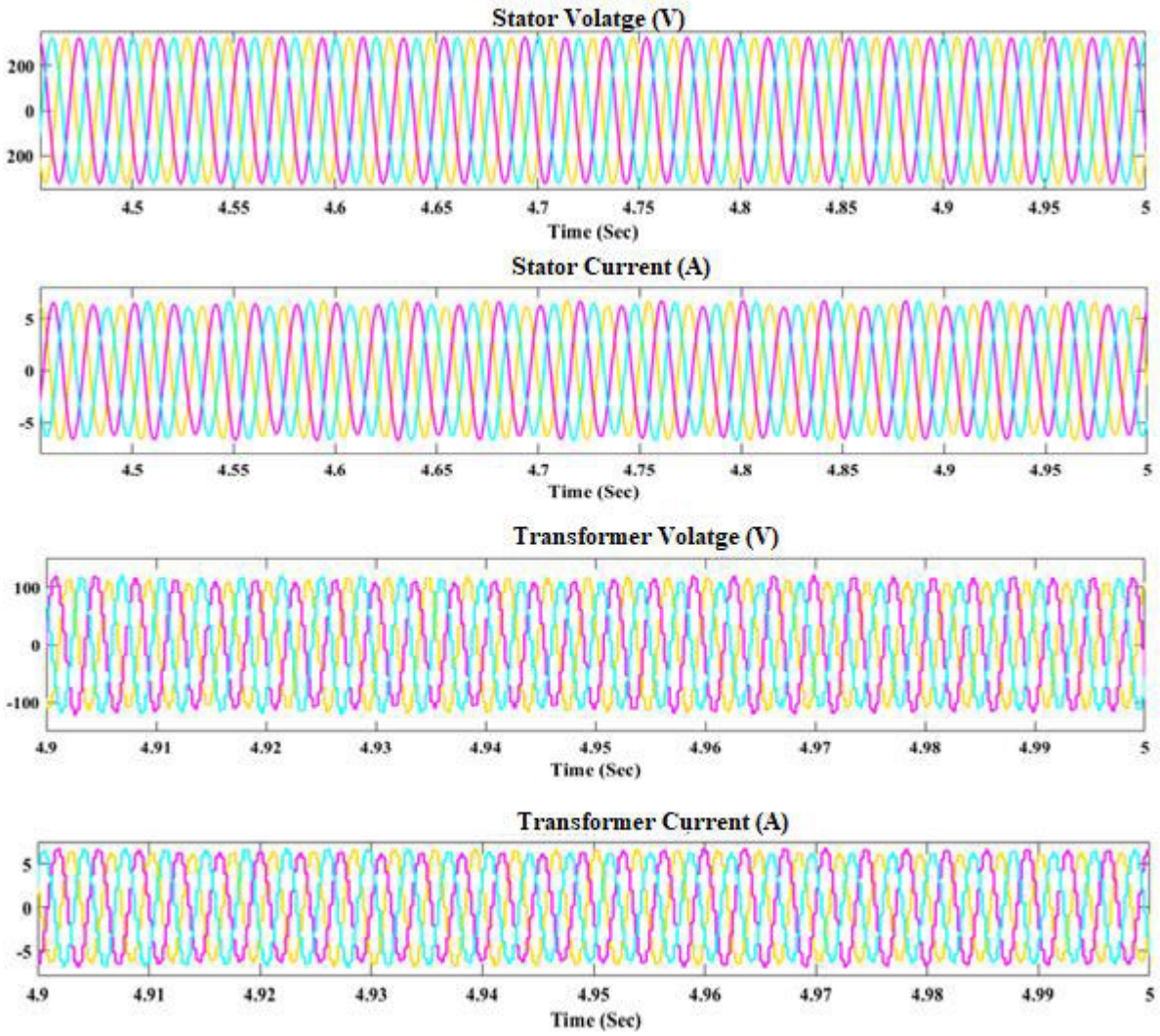

FIGURE 15. Zoomed response of stator voltage and current with FOPI controller.

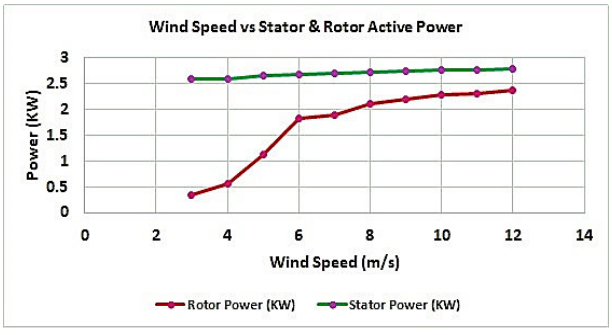

FIGURE 16. Wind speed and output power with PI controller.

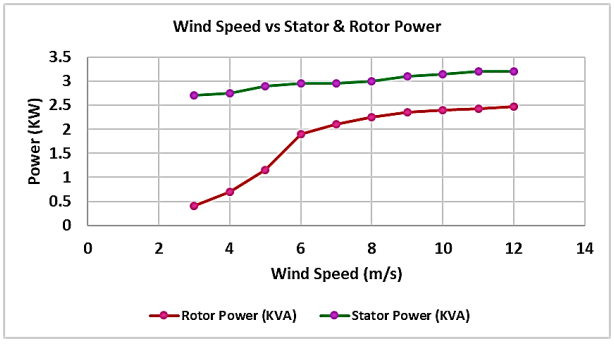

FIGURE 17. Wind speed and output power with FOPI controller.

The total output power obtained with conventional PI controller and proposed FOPI controller is plotted in Figure 18. It has been observed that the results obtained through the real time simulation through software synchronization mode and the hardware connected hardware synchronization mode are very much comparable and promising as compared to the offline MATLAB simulation results. Also it is evident from the comparison of output power efficiency with conventional

TABLE 2. Summary of related work.

Sr. No.	Reference No.	Year	Method / Technique used	Advantages / Findings	Hardware/Software Tools used
1	11	2020	probabilistic feedforward NN (PFFNN), multi-layer perceptron feedforward NN (MLPFFN) and radial basic function feedforward NN (RBFFN)	Effective in with linear model of WT Need to test with non-linear model	MATLAB
2	12	2018	Sliding Mode Field oriented control	High performance with robust uncertain systems	MATLAB/ Simulink and RT-LAB
3	13	2013	Discrete SMC	Does not require synchronous coordinate frame, Improved power quality	MATLAB
4	14	2015	Internal Model Control based SVO	Stability improvement with PI tuning	MATLAB
5	15	2017	Fractional order terminal SMC	Faster transient response and minimum chattering	MATLAB/Simulink
6	16	2023	Robust protection technology under LVRT condition	Enhanced LVRT Capability	PSCAD/EMTDC
7	17	2017	Direct Vector control and FSMC	Reduced harmonics with FSMC	MATLAB/Simulink
8	18	2017	PI-Hysteresis based Voltage and Frequency Control	Robust under different operating conditions	dSPACE DS1104
9	19	2016	Second order SMC	Robust against uncertainties and parametric variations, need tuning revaluation	OPAL RT real time simulator OP5600
10	20	2018	Coordinated control using extended equal area criteria	Improved transient stability with enhanced control economy	DIgSILENT
11	21	2023	Event triggered SMC, dynamic voltage restorer	Effective in fault mitigation Reduces harmonics distortion	dSPACE MicroLabBox
12	22	2018	LQR-Optimal preview control (OPC)	Improved steady-state stability and steady-state error	MATLAB/Simulink and Opal-RT

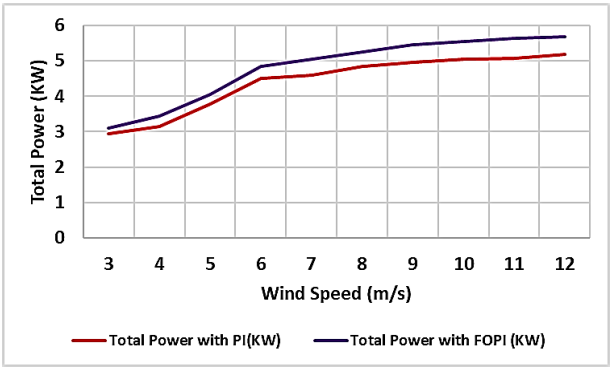

FIGURE 18. Total output power with PI and proposed FOPI.

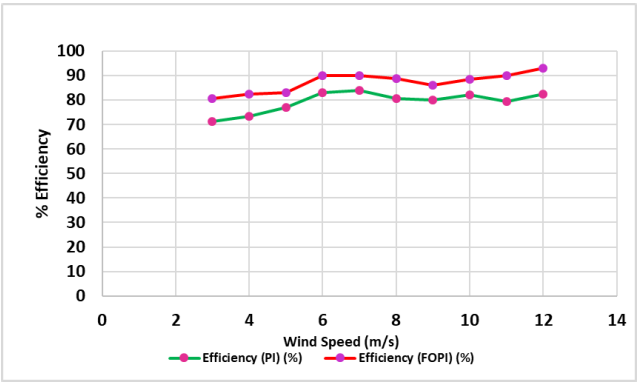

FIGURE 19. Output power efficiency with PI and FOPI controller.

PI controller and that of proposed fractional order PI controller that the FOPI controller gives much better efficiency as compared to the conventional controller. Also it is observed from the stator and rotor power output with both the controller schemes that the DFIG has been advantageous in case wind turbine application as the rotor power is less than that of the stator power always and so require the lower capacity power electronics converters. Also it has been observed form the experimental results that decoupled PQ control is possible with the conventional and proposed controller schemes. The DC link voltage also remains constant though the wind speed and so the generator speed is changed.

Table 1 furnishes the output power efficiency of laboratory based DFIG with conventional and proposed control strategies applied with real time digital simulator. The efficiency for both the controllers has been plotted in Figure 19 for comparison purpose. As demonstrated in previous subsection, the tracking performance, transient response and decoupled control with proposed fractional order PI controller is much better than that of the conventional PI controller. These properties of the fractional order controller cause enhanced performance and increased efficiency when used in real time simulation environment.

The conventional PI controller have certain limitations when used in power converter control such as sluggish response, issues in handling the nonlinearity, lack of robustness in handling the parameter uncertainty, etc. The proposed fractional order controller gives better close loop response with reduced overshoot and enhanced robustness to parameter uncertainty in nonlinear systems. Extended control loop tuning flexibility is possible with FOPID controllers, which can increase control performance—especially for intricate

TABLE 3. DFIG parameters.

Parameter	Value
R_s/ph	0.282ohm
R_r/ph	0.197ohm
Stator leakage Reac/ph	0.532ohm
Rotor leakage Reac/ph	0.911ohm
No load current	8.5A
Output Power	6.0KVA
Frequency	50 Hz
Rotor Voltage	415V
Connection	Y
Efficiency	90%
Speed	1500 rpm

and nonlinear systems. Tuning flexibility, improved damping response with memory capability and adaptability are some of the important advantages of FOPI over conventional PI controller which may lead to improved efficiency and better performance.

Further the proposed controller performance is compared with that of the fractional order MPPT [46] control of DFIG based WT system and observed better tracking active and reactive power tracking performance as well as reduced steady state error. Furthermore, though there are fairly many other types of fractional order controllers designed and implemented as studied in the literature are either simulated only in software simulation or on the laboratory based test simulators with varying simulation environments, only few are tested with hardware-in-loop simulation environment with real time digital simulator and hence their performance has not been adequately investigated and compared.

V. CONCLUSION

The proposed fractional order control method was implemented in real time utilizing OPAL-RT's real time digital simulator OP4510. The effectiveness of the control strategy was then validated by experiments conducted on a laboratory-based DFIG testbed. The conventional and proposed control systems were implemented using a real-time simulator, and a comparison was made between the simulation and experimental results. The demonstrated results clearly demonstrate that the response of the suggested controller is smoother and superior in comparison to the conventional controller. Additionally, the generated results exhibit a higher level of discreteness compared to the offline MATLAB simulation. The controller subsequently conducted real-time hardware-in-the-loop experimental validation on the doubly-fed induction generator (DFIG) experimental setup and observed the output power efficiency. The efficiency of the suggested controller has been observed to range from 80 to 93 percent when subjected to wind speed variations ranging from 3 m/s to 12 m/s.

TABLE 4. Induction motor drive parameters.

Parameter	Value
No load current	8.5A
Power	7.5kW
Frequency	50 Hz
Power factor	0.8
Voltage	415V
Connection	Delta
Efficiency	88%
Speed	1450 rpm

APPENDIX

A. SUMMARY OF RELATED WORK

See Table 2.

B. DFIG PARAMETERS

See Table 3.

C. PARAMETERS OF INDUCTION MOTOR DRIVE

See Table 4.

ACKNOWLEDGMENT

The authors extend their appreciation to the Researchers Supporting Project at King Saud University, Riyadh, Saudi Arabia, for funding this research work through the project number RSP2023R278. The authors extend their appreciation to the Researchers Supporting Project at Universiti Teknologi Malaysia (UTM), Malaysia (UTMFR: Q.J130000.3823.23H05 and UTMER: Q.J130000.3823.31J06). The authors extend their appreciation to Intelligent Prognostic Private Limited Delhi, India for providing technical support in this research work.

REFERENCES

[1] REN21. (2022). *Renewables 2022 Global Status*. [Online]. Available: https://www.ren21.net/gsr-2022/
[2] V. Tank, J. Bhutka, and T. Harinarayana, "Wind energy generation and assessment of resources in India," *J. Power Energy Eng.*, vol. 4, no. 10, pp. 25–38, 2016, doi: 10.4236/jpee.2016.410002.
[3] S. B. Ahmed, H. Malik, S. M. Ayob, N. R. N. Idris, A. Jusoh, and F. P. G. Márquez, "Data resource library for renewable energy prediction/forecasting," in *Renewable Power for Sustainable Growth* (Lecture Notes in Electrical Engineering), vol. 1086, H. Malik, S. Mishra, Y. R. Sood, A. Iqbal, T. S. Ustun, Eds. Singapore: Springer, 2024, doi: 10.1007/978-981-99-6749-0_7.
[4] *Renewables 2022 Analysis and Forecast to 2027*, IEA, Paris, France, 2022.
[5] *Gwec—Global Wind Report 2018*, Global Wind Energy Council (GWEC), Brussels, Belgium, 2019.
[6] D. K. Sharma and S. P. Shukla, "Performance evaluation of SFIG and DFIG based wind turbines," *J. Comput. Inf. Syst.*, vol. 15, no. 2, pp. 45–53, 2019.
[7] H. Malik, S. Mishra, Y. R. Sood, A. Iqbal, and T. S. Ustun, *Renewable Power for Sustainable Growth* (Lecture Notes in Electrical Engineering). Singapore: Springer, 2024, p. 1023, doi: 10.1007/978-981-33-4080-0.
[8] D. Zhou, G. Zhang, and F. Blaabjerg, "Optimal selection of power converter in DFIG wind turbine with enhanced system-level reliability," *IEEE Trans. Ind. Appl.*, vol. 54, no. 4, pp. 3637–3644, Jul. 2018, doi: 10.1109/TIA.2018.2822239.
[9] A. K. Singh and A. Saxena, "A novel neuro-fuzzy control scheme for wind-driven DFIG with ANN-controlled solar PV array," *Environ., Develop. Sustainability*, vol. 22, no. 7, pp. 6605–6626, Oct. 2020, doi: 10.1007/s10668-019-00502-5.

[10] G. S. Kaloi, J. Wang, and M. H. Baloch, "Active and reactive power control of the doubly fed induction generator based on wind energy conversion system," *Energy Rep.*, vol. 2, pp. 194–200, Nov. 2016, doi: 10.1016/j.egyr.2016.08.001.

[11] D. Khan, J. Ahmed Ansari, S. Aziz Khan, and U. Abrar, "Power optimization control scheme for doubly fed induction generator used in wind turbine generators," *Inventions*, vol. 5, no. 3, p. 40, Aug. 2020, doi: 10.3390/inventions5030040.

[12] L. Djilali, E. N. Sanchez, and M. Belkheiri, "Real-time implementation of sliding-mode field-oriented control for a DFIG-based wind turbine," *Int. Trans. Electr. Energy Syst.*, vol. 28, no. 5, p. e2539, May 2018, doi: 10.1002/etep.2539.

[13] V. N. Pande, U. M. Mate, and S. Kurode, "Discrete sliding mode control strategy for direct real and reactive power regulation of wind driven DFIG," *Electric Power Syst. Res.*, vol. 100, pp. 73–81, Jul. 2013, doi: 10.1016/j.epsr.2013.03.001.

[14] D. Y. Shingare and T. K.. S. Kumar, "Stability of DFIG stator voltage oriented control design based on internal model control," in *Proc. IEEE Int. Conf. Signal Process. Inform., Commun. Energy Syst.*, Feb. 2015, pp. 1–5, doi: 10.1109/SPICES.2015.7091516.

[15] N. Ullah, M. A. Ali, A. Ibeas, and J. Herrera, "Adaptive fractional order terminal sliding mode control of a doubly fed induction generator-based wind energy system," *IEEE Access*, vol. 5, pp. 21368–21381, 2017, doi: 10.1109/ACCESS.2017.2759579.

[16] L. Van Dai, "A novel protection method to enhance the grid-connected capability of DFIG based on wind turbines," *IETE J. Res.*, pp. 1–17, Jan. 2023, doi: 10.1080/03772063.2022.2163925.

[17] H. Benbouhenni, "Comparative study between direct vector control and fuzzy sliding mode controller in three-level space vector modulation inverter of reactive and active power command of DFIG-based wind turbine systems," *Int. J. Smart Grid*, vol. 2, no. 4, pp. 188–196, 2018.

[18] M. Saci. Chabani, M. T. Benchouia, A. Golea, and R. Boumaaraf, "Implementation of direct stator voltage control of stand-alone DFIG-based wind energy conversion system," in *Proc. 5th Int. Conf. Electr. Eng.-Boumerdes (ICEE-B)*, Oct. 2017, pp. 1–6, doi: 10.1109/ICEE-B.2017.8192060.

[19] A. Merabet, K. T. Ahmed, H. Ibrahim, and R. Beguenane, "Implementation of sliding mode control system for generator and grid sides control of wind energy conversion system," *IEEE Trans. Sustain. Energy*, vol. 7, no. 3, pp. 1327–1335, Jul. 2016, doi: 10.1109/TSTE.2016.2537646.

[20] M. Zhou, Z. Dong, H. Li, C. Gan, G. Li, and Y. Liu, "Coordinated control of DFIG based wind farms and SGs for improving transient stability," *IEEE Access*, vol. 6, pp. 46844–46855, 2018, doi: 10.1109/ACCESS.2018.2866252.

[21] M. N. Musarrat, A. Fekih, M. A. Rahman, M. R. Islam, and K. M. Muttaqi, "Event-triggered SMC-based FRT approach for DFIG-based wind turbines equipped with DVR with high frequency isolation," *IEEE J. Emerg. Sel. Topics Power Electron.*, vol. 11, no. 3, pp. 2661–2671, Jun. 2023, doi: 10.1109/JESTPE.2022.3233349.

[22] B. Subudhi and P. S. Ogeti, "Optimal preview stator voltage-oriented control of DFIG WECS," *IET Gener., Transmiss. Distrib.*, vol. 12, no. 4, pp. 1004–1013, Feb. 2018, doi: 10.1049/iet-gtd.2016.2027.

[23] S. Karad and R. Thakur, "Recent trends of control strategies for doubly fed induction generator based wind turbine systems: A comparative review," *Arch. Comput. Methods Eng.*, vol. 28, no. 1, pp. 15–29, Jan. 2021, doi: 10.1007/s11831-019-09367-3.

[24] S. Sharma, S. Gupta, M. Zuhaib, V. Bhuria, H. Malik, A. Almutairi, A. Afthanorhan, and M. A. Hossaini, "A comprehensive review on STATCOM: Paradigm of modeling, control, stability, optimal location, integration, application, and installation," *IEEE Access*, vol. 12, pp. 2701–2729, 2024, doi: 10.1109/ACCESS.2023.3345216.

[25] N. Bouchiba, A. Barkia, L. Chrifi-Alaoui, S. Drid, S. Sallem, and M. B. A. Kammoun, "Real-time integration of control strategies for an isolated DFIG-based WECS," *Eur. Phys. J. Plus*, vol. 132, no. 8, pp. 134–144, Aug. 2017, doi: 10.1140/epjp/i2017-11617-3.

[26] A. Beddar, H. Bouzekri, B. Babes, and H. Afghoul, "Real time implementation of improved fractional order proportional-integral controller for grid connected wind energy conversion system," *Revue Roumaine Des Sciences Techn. Serie Electrotechnique et Energetique*, vol. 31, no. 4, pp. 402–407, 2016.

[27] H. Pang, F. Zhang, H. Bao, G. Joós, W. Wang, W. Li, L.-A. Gregoire, and X. Zhai, "Simulation of modular multilevel converter and DC grids on FPGA with sub-microsecond time-step," in *Proc. IEEE Energy Convers. Congr. Expo. (ECCE)*, Oct. 2017, pp. 2673–2678, doi: 10.1109/ECCE.2017.8096503.

[28] A. K. Singh and R. Thakur, "Real time simulation of IEEE 9 bus system for fault analysis using transient response," in *Advanced Informatics for Computing Research*, vol. 956. Singapore: Springer, 2019.

[29] A. A. Bhandakkar and L. Mathew, "Real-time-simulation of IEEE-5-bus network on OPAL-RT-OP4510 simulator," *IOP Conf. Ser., Mater. Sci. Eng.*, vol. 331, no. 1, 2018, Art. no. 012028, doi: 10.1088/1757-899X/331/1/012028.

[30] F. Alvarez-Gonzalez, A. Griffo, B. Sen, and J. Wang, "Real-time hardware-in-the-loop simulation of permanent-magnet synchronous motor drives under stator faults," *IEEE Trans. Ind. Electron.*, vol. 64, no. 9, pp. 6960–6969, Sep. 2017.

[31] S. Krishnama Raju and G. N. Pillai, "Design and implementation of type-2 fuzzy logic controller for DFIG-based wind energy systems in distribution networks," *IEEE Trans. Sustain. Energy*, vol. 7, no. 1, pp. 345–353, Jan. 2016.

[32] J. Liang, W. Qiao, and R. G. Harley, "Feed-forward transient current control for low-voltage ride-through enhancement of DFIG wind turbines," *IEEE Trans. Energy Convers.*, vol. 25, no. 3, pp. 836–843, Sep. 2010, doi: 10.1109/TEC.2010.2048033.

[33] K. Kerrouche, A. Mezouar, and K. Belgacem, "Decoupled control of doubly fed induction generator by vector control for wind energy conversion system," *Energy Proc.*, vol. 42, pp. 239–248, Jan. 2013, doi: 10.1016/j.egypro.2013.11.024.

[34] Y. M. Alsmadi, L. Xu, F. Blaabjerg, A. J. P. Ortega, A. Y. Abdelaziz, A. Wang, and Z. Albataineh, "Detailed investigation and performance improvement of the dynamic behavior of grid-connected DFIG-based wind turbines under LVRT conditions," *IEEE Trans. Ind. Appl.*, vol. 54, no. 5, pp. 4795–4812, Sep. 2018, doi: 10.1109/TIA.2018.2835401.

[35] X. Lin, K. Xiahou, Y. Liu, and Q. H. Wu, "Design and hardware-in-the-loop experiment of multiloop adaptive control for DFIG-WT," *IEEE Trans. Ind. Electron.*, vol. 65, no. 9, pp. 7049–7059, Sep. 2018, doi: 10.1109/TIE.2018.2798566.

[36] H. Bakir, A. Merabet, and A. A. Kulaksiz, "Control in the DFIG-based wind energy system using OPAL-RT," *Eur. J. Sci. Technol.*, vol. 2020, pp. 373–379, Oct. 2020, doi: 10.31590/ejosat.806091.

[37] I. Petras, "Fractional-Order Systems," in *Fractional-Order Nonlinear Systems* (Nonlinear Physical Science). Berlin, Germany: Springer, 2011, pp. 43–54, doi: 10.1007/978-3-642-18101-6_3.

[38] Y. Chen, "Applied fractional calculus in controls and signal processing," in *Proc. Amer. Control Conf.*, St. Louis, MO, USA, 2009, pp. 34–35, doi: 10.1109/ACC.2009.5159794.

[39] N. Kumar, M. A. Alotaibi, A. Singh, H. Malik, and M. E. Nassar, "Application of fractional order-PID control scheme in automatic generation control of a deregulated power system in the presence of SMES unit," *Mathematics*, vol. 10, no. 3, p. 521, 2022, doi: 10.3390/math10030521.

[40] T. Mahto, R. Kumar, H. Malik, S. M. S. Hussain, and T. S. Ustun, "Fractional order fuzzy based virtual inertia controller design for frequency stability in isolated hybrid power systems," *Energies*, 14, p. 1634, Mar. 2021, doi: 10.3390/en14061634.

[41] A. Tepljakov, E. Petlenkov, and J. Belikov, "FOMCOM: A MATLAB toolbox for fractional-order system identification and control," *Int. J. Microelectron. Comput. Sci.*, vol. 2, no. 2, pp. 51–62, 2021.

[42] E. A. Gonzalez, V. Alimisis, C. Psychalinos, and A. Tepljakov, "Design of a generalized fractional-order PID controller using operational amplifiers," in *Proc. 25th IEEE Int. Conf. Electron., Circuits Syst. (ICECS)*, Dec. 2018, pp. 253–256.

[43] A. Tepljakov, E. Petlenkov, and J. Belikov, "Closed-loop identification of fractional-order models using FOMCON toolbox for MATLAB," in *Proc. Bienn. Balt. Electron. Conf.*, 2015, pp. 213–216, doi: 10.1109/BEC.2014.7320594.

[44] A. W. Saif, K. B. Gaufan, S. El-Ferik, and M. Al Dhaifallah, "Fractional order sliding mode control of quadrotor based on fractional order model," *IEEE Access*, vol. 11, pp. 79823–79837, 2023, doi: 10.1109/ACCESS.2023.3296644.

[45] C. Dufour, "Highly stable rotating machine models using the state-space-nodal real-time solver," in *Proc. IEEE Work. Complex. Eng.* , Oct. 2018, pp. 1–10, doi: 10.1109/CompEng.2018.8536236.

[46] S. G. Karad and R. Thakur, "Fractional order controller based maximum power point tracking controller for wind turbine system," *Int. J. Electron.*, vol. 109, no. 5, pp. 875–899, May 2022.